Annals of Nuclear Energy 142 (2020) 107424

Contents lists available at ScienceDirect

Annals of Nuclear Energy

journal homepage: www.elsevier.com/locate/anucene

Physical anomaly detection and identification using Cerenkov radiation

Jason A. Hearne *, Pavel V. Tsvetkov

Texas A&M University, Department of Nuclear Engineering, United States

ARTICLE INFO

Article history:
Received 26 November 2019
Received in revised form 17 February 2020
Accepted 23 February 2020
Available online 5 March 2020

Keywords:
Cerenkov radiation
TRIGA
Coolant channel blockage
Reactor instrumentation

ABSTRACT

This paper demonstrates the potential use of a method of power profile determination using Cerenkov radiation to detect and identify some physical anomalies in a reactor. Specifically, the blockage of a coolant channel in a square lattice TRIGA reactor is investigated. The ability to quickly detect some blockages is demonstrated. A method is developed through which the blocked channel and approximate size and location of the blockage within the channel can be found by comparing the detectable visible Cerenkov radiation at multiple locations above the core. An example blockage scenario is analyzed, and its location determined from the information obtainable from Cerenkov light detection viewpoints above the core.

1. Introduction

One application of a Cerenkov radiation based power profile determination method is the ability to quickly detect and pinpoint some physical anomalies in the reactor, such as a coolant channel blockage. In this study, a previously developed method of using Cerenkov radiation to measure the 2D and 3D spatial power profile in a reactor (Hearne and Tsvetkov, 2020a,b,c) (Hearne and Tsvetkov, 2020a,b,c) is applied to the detection of a blocked coolant channel, and altered to have the ability to determine the approximate size and location of the blockage within the channel. If such a power profile measuring system were implemented in a reactor, channel blockage detection is one additional beneficial feature that is investigated here.

The partial or complete blockage of a flow channel in a reactor can cause fuel damage due to a reduction in the cooling of fuel elements. Damage from flow channel blockage during operation (Keller, 1962) can be mitigated if the block is detected quickly and appropriate action is taken before fuel damage occurs. Most of the coolant channel blockage analysis that can be found in literature focuses on the effects of the block on fuel temperature rises and coolability (Schultheiss, 1987) (Adorni, et al., 2005) (Son, et al., 2015); most of the more recent analyses are CFD simulations (Salama and El-Morshedy, 2012) (Salama, 2012) (Chance, 2014) (Ma, et al., 2018). The detection of coolant channel blockages during operation is generally done by detecting secondary effects, such as temperature fluctuations (Greef, 1979), coolant flow decreases (Keller, 1962), neutronic effects caused by the boiling and voiding of coolant in the blocked channels (de Vires, et al., 1990) (Turkcan, et al., 1992). A method for monitoring cladding blockage based upon gamma production in the blocking material from neutron capture has also been proposed (De Volpi, et al., 1975). A partial blockage of a channel may not be detected until it is large enough to significantly disturb core, after which damage may have already occurred. Some pool and tank type reactors already use a camera above the core to qualitatively detect channel blockages. The system proposed here would function in a similar way, using visible light to automatically detect blocks in addition to determining the spatial power profile in the core. Faster detection of a block could allow for action to be taken sooner to mitigate negative consequences.

2. Overview of Cerenkov power monitoring system

The concept for a method for the use of Cerenkov radiation detection for spatial power profile determination can be found in (Hearne and Tsvetkov, 2020a,b,c). A short overview of the method is provided here. Photon detectors or cameras can be placed a significant distance above the coolant channels in a reactor to measure the amount of Cerenkov light produced in the channel that reaches the detector. An MCNP model of a square lattice TRIGA reactor is used to tally the spatial and energy dependent electron fluxes in coolant channels. A response function generated in (Hearne and Tsvetkov, 2020a,b,c) is then used to convert the tallied electron fluxes to the detectable visible light from Cerenkov above the core. The response function was generated using MCNP 6.1.1 Beta's Cerenkov production and visible photon tracking feature. It

* Corresponding author.
E-mail address: jasonhearne@email.tamu.edu (J.A. Hearne).

https://doi.org/10.1016/j.anucene.2020.107424
0306-4549/

takes the electron flux within the coolant channel in 16 spatial bins and 23 electron energy bins, and converts it into the total visible light above the core resulting from the tallied electrons. The amount of Cerenkov radiation coming from each channel is strongly correlated with the power density in the surrounding pins, allowing a map of the Cerenkov light coming from each coolant channel to be used as a source of information about the 2D power profile in the reactor. Anomalies that cause significant changes in the power profile can be detected. An extension of the power profile determination method involves using shadowing effects from multiple detector viewpoints above a single coolant channel to obtain information about the axial tilt in the reactor power (Hearne and Tsvetkov, 2020a,b,c). The shadowing effects use a square channel approximation and second detector offset location that has a 7 cm lateral offset from the channel at a position 2 m above the core's axial centerline such that the portion of the channel that is visible varies linearly with the axial position within the channel, ranging from 100% for the top of the channel to 0% at the bottom. The square channel approximation allows for the simplified geometrical treatment of shadowing, resulting in a linear dependence of shadowing on the axial position within the channel. The position of 2 m for the simulated detection surface was chosen as a representative location. The relatively close 2 m distance from the midplane had the advantage of more particles reaching the tallies in the MCNP models, easing constraints on computation time. For a different distance from the core, either a new response function would need to be generated, or a correction for the distance would need to be made. In all cases the total visible Cerenkov light is used; no attempt to further distinguish the energy spectrum of the detected light is made.

The array of detection points here is idealized, with a detection point directly above every coolant channel and offset detection points the exact lateral distance from the line above each channel. A real system would likely use fewer detection points, with differing shadowing corrections for each, or it could incorporate a system of either reflectors or fiber optic light guides to direct the light from multiple channels to a smaller number of multichannel detectors.

3. Coolant channel blockage analysis

One feature of a Cerenkov power monitoring system is the ability to quickly detect and pinpoint the location of some types of coolant channel blockages. Any obstruction of the middle or upper portion of a channel will cause an immediate change in the amount of Cerenkov light detected above the channel. This could be automatically detected based upon the quantitative change in light coming from the obstructed channel, potentially triggering a reactor trip or more likely an alarm to alert operators to what has occurred. The time required for detection is could be as short as a second or less, as Cerenkov detection based reactor power measurements have been used to characterize reactor pulses, which occur on timescales of milliseconds (Holschuh and Marcum, 2019). The complete or partial blockage of a coolant channel will often have little to no immediate effect on the neutron or gamma flux in the core, and will only be detectable through conventional gamma or neutron measurements if the decrease in local cooling causes significant temperature feedback effects. Coolant temperature and flow measurements may be able to detect differences caused by a blockage, depending on where the block occurs relative to the flow monitors, but it is not a guarantee and the temperature measurements have a longer delay time. The example channel blockage analyzed here demonstrates the ease with which the visual information based power profile reconstruction method can locate a coolant channel obstruction. A blockage at the bottom of the channel, furthest from the Cerenkov light detectors would not immediately cause a large change in the light with this design; however, if it progresses to causing boiling in the channel, this would be instantly detectable. This analysis is restricted to blockages that occur above the bottom portion of the core and that do not cause boiling in the channel.

To simulate a channel obstruction, the code used to post process the MCNP output decks was modified to include this ability. The code takes an input for the blocked coolant channel, at a specified height (which axial segment the block occurs in), and the portion of the channel that is blocked. It then calculates the blocked Cerenkov and blocked axial offset by reducing the contribution of all segments below the blockage to the total Cerenkov by the blockage factor. So for a full blockage at the midplane, all segments in the bottom half of the channel would contribute nothing to the total. For a 50% blockage, the segments below it would provide 50% of their normal contribution.

A blockage is simulated in channel 4,4 of the reactor. This channel is between fuel pin 4,4, pin 4,5, pin 5,4 and pin 5,5. The blockage is at z = 0 cm, the core midplane, above axial segment 9 in the electron tally. It is a complete blockage, so the segments below it (9–16) have their Cerenkov contribution multiplied by zero. The resulting Cerenkov total is vastly decreased in channel 4,4 to 48.3% of its original value. The altered Cerenkov map can be seen in Fig. 1, with units of visible Cerenkov photons above the core per source neutron in the MCNP model of the reactor. A plot of the difference using the same scaling as previous 2D difference plots can be seen in Fig. 2. The magnitude of the change is approximately 1.2e−7, which greatly exceeds the scale of the plot with a maximum magnitude of 5e−8. This would create a large signal in any monitoring system that could not be caused by any difference in the neutronics of the core, and thus can be clearly identified as either a blockage or a detector failure. A 52% blockage at the top of the fuel would cause the same effect in the total Cerenkov, so the offset information would also be needed to distinguish between the two different blockage scenarios.

The presence of a blockage also causes a large change in the axial Cerenkov tilt in the affected channel. In Fig. 3, the axial offset for each channel can be seen with the blocked channel being the only one with a positive offset. A rescaled version of the plot can be seen in Fig. 4. As in (Hearne and Tsvetkov, 2020a,b,c) the adjusted axial offset ratio, or absolute tilt is calculated using Eqs. (1) and (2),

$$\textit{Axial offset ratio} = \textit{flux tilt ratio} = \frac{\textit{Cerenkov detection at offset position}}{\textit{Cerenkov directly above channel}} \tag{1}$$

$$\textit{Adjusted offset ratio} = \textit{absolute tilt} = \textit{flux tilt ratio} - \textit{symmetric tilt ratio} \tag{2}$$

The symmetric tilt ratio is the flux tilt ratio for a channel in an infinite reflected lattice of pins with no control rods or other axially shifting phenomenon. It is used as a normalization to remove the apparent upwards shifting effect caused by the fact that the top of the channel is closer to the detection point, causing photons formed near the top to experience less spreading and attenuation. The symmetric tilt ratio is 0.5248. Due to the presence of control rods above and in the top portion of the core, the absolute tilt in the reactor should almost always be negative.

The offset in channel 4,4 is 0.682, corresponding to an adjusted offset of 0.157. This upwards tilt occurs because the Cerenkov detection directly above the channel was affected more than the offset location. The direct Cerenkov decreases from 2.42e−7 to 1.17e−7, for a 51.7% decrease, while the offset decreases from 1.20e to 7 to 7.99e−8, a 33.2% decrease. This information makes

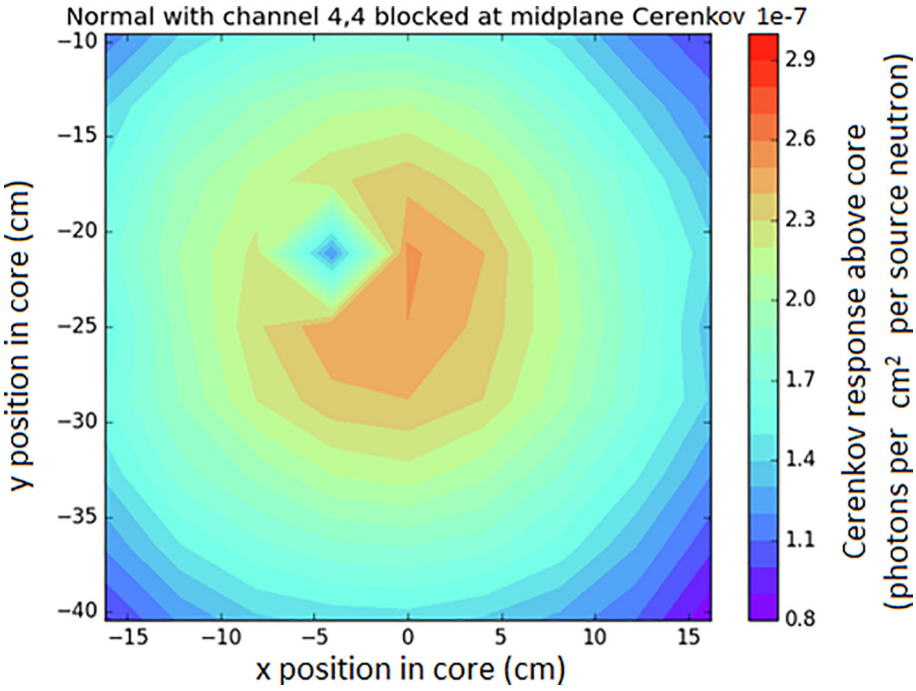

Fig. 1. Total Cerenkov above core with channel 4,4 blocked 100% at midplane.

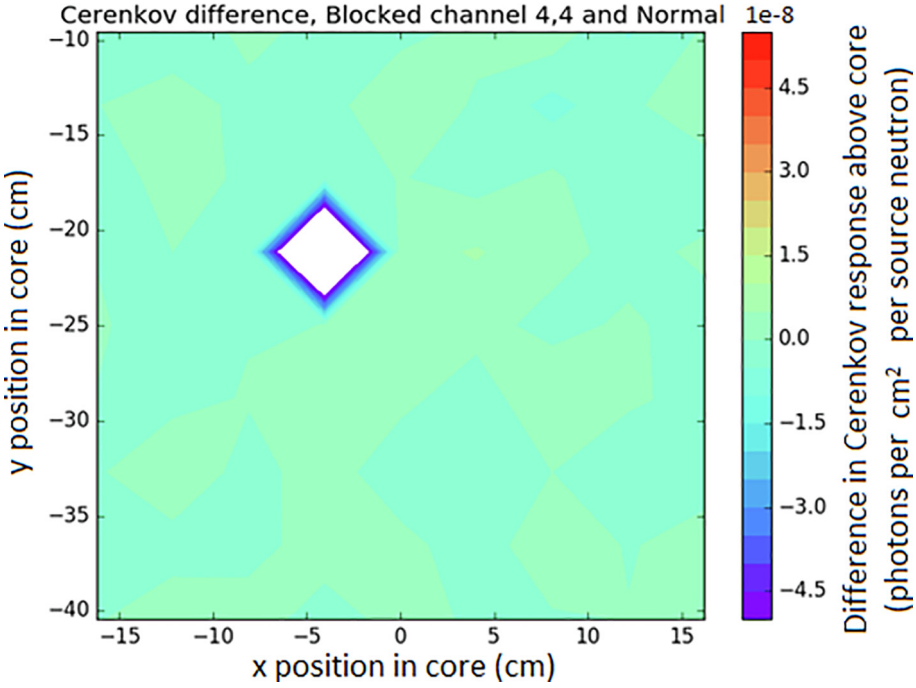

Fig. 2. Cerenkov difference above core with a blockage in channel 4,4.

a detector failure in the detector above the channel a highly unlikely scenario, because two separate detectors are experiencing a major change.

To use the offset information shown above to identify the cause as a complete block near the midplane of the core, rather than a partial block near the top, it may be necessary to have more than one offset viewpoint. This is because a partial block could have a different effect on the offset viewpoint based upon its location within the channel. A partial block at the top of the channel on the side near the offset viewpoint would have a greater effect, while one opposite to the viewpoint would have a reduced effect; anything in between is also possible. If the assumption were made that a partial block would cause the same fractional reduction to the Cerenkov contributions below it for the direct viewpoint and the offset viewpoint, then a partial block near the top could be ruled out in by this information because it would cause no change in the tilt ratio. Multiple offset viewpoints in different directions with similar offset distances could be used to fix this. Instead of one offset viewpoint in the direction of a pin, four viewpoints, one in the direction of each pin neighboring the channel can be

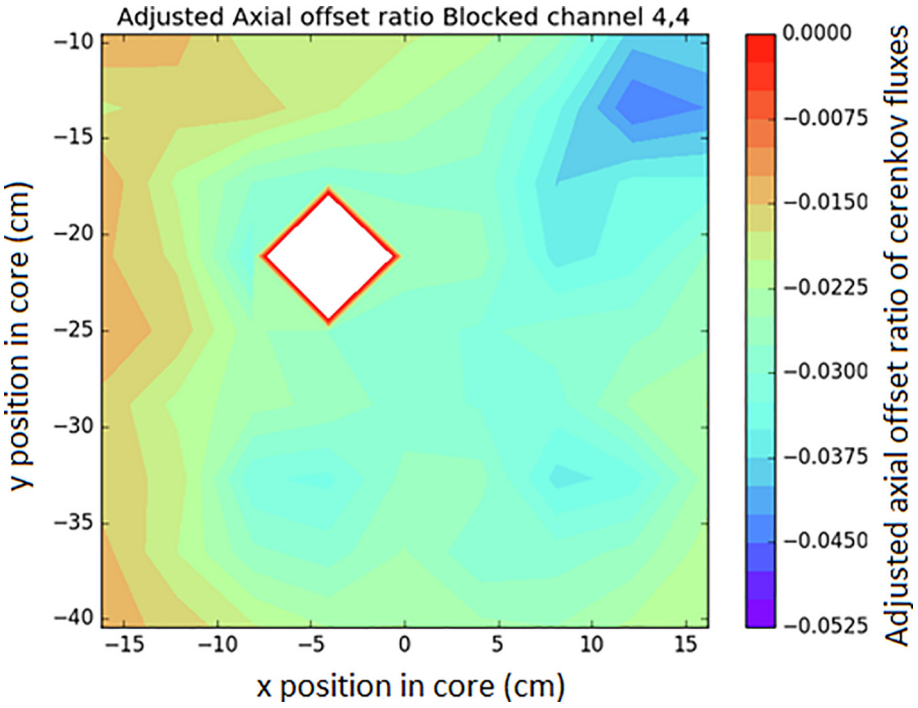

Fig. 3. Axial tilt map of core with a 100%blockage at the core midplane in channel 4,4. White space is where the tilt is outside of the previously used range.

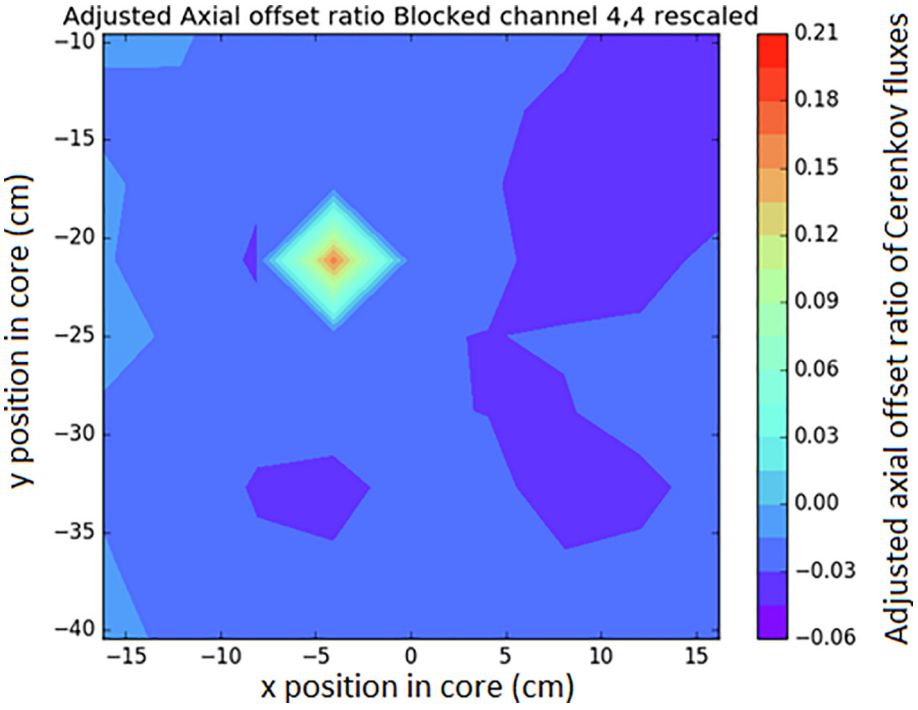

Fig. 4. Rescaled plot of axial Cerenkov tilt with blocked channel. The large positive tilt in the affected channel stands out compared to the rest of the core.

used, as seen in Fig. 5. If the amount of light detected from a channel for each of four offset viewpoints were averaged, the assumption of an equal change to the direct viewpoint would be valid. Also, any major differences in the results detected by the different offsets can be used to determine which side of the channel a partial block is located. If the 4 offset viewpoints are affected asymmetrically by a partial block near the top of the channel, the block will be laterally positioned near the most affected offset viewpoint, because it will block the view of a larger portion of the channel. If the partial block is near the middle of the core, it would be laterally located opposite to the most affected offset, because in the nearest viewpoint, the blockage would be in the region already shadowed by the pin. This is demonstrated in two simple cases involving a 50% block covering one side of the channel either at the top of the channel or at the midplane, seen in Fig. 6, with the corresponding effects on the adjacent and opposite offset

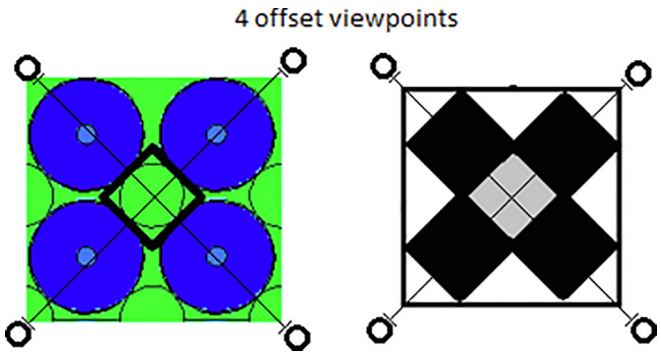

Fig. 5. Pin geometry and square channel approximation using four offset viewpoints, one in the direction of each neighboring pin.

viewpoints. A block near the top cuts out 3/8th of the total channel volume, or 3/4th of the normally viewable channel volume for the nearby offset viewpoint, while only blocking 1/8th of the total volume for the opposite viewpoint. The partial midplane block has no effect on the near viewpoint, but still blocks 1/8th of the total channel volume for the opposite offset. For blockages that are not directly placed towards an offset viewpoint, a combination of all 4 would be used. An example of this is shown in the following section.

4. Example blockage detection and location determination

An example case of the detection and location of a partial blockage within a channel using offset viewpoints is demonstrated here. For this example, there is an approximately 50% block at the core midplane on one side of channel 5,3. The block is shown in Fig. 7, along with the corresponding approximation used for the model of the Cerenkov detectors' response. The block is approximated as covering one side of the square coolant channel at the midplane.

The normal level of Cerenkov without any blockage detected directly above channel 5,3 is 2.363E−7, in units of Cerenkov photons per cm^2 per source neutron, as output by MCNP. This is altered by reducing the contribution of the lower half of the channel, segments 1 through 8, by 50%, due to the partial blockage at z = 0 cm. The resulting measurement directly above is 1.762E−7. This is a decrease of 25.4%, which is reasonable given that 1/4th of the total channel volume is blocked and that the flux in most of the core is tilted downwards slightly, such that the slightly increased importance of the upper regions is countered by the higher prevalence of radiation in the lower regions.

The four offset viewpoints have different reactions to the blockage. For convenience here, they will be referred to North, South, East and West, with the block located on the southern side of the core, as labeled in Fig. 7. With no block, all four offset viewpoints should have approximately the same Cerenkov measurements of 1.174E−7, corresponding to a tilt ratio of 0.4968. Subtracting 0.5248 for normalization gives an adjusted tilt ratio of -0.028, corresponding to a slight downward tilt, as seen in previous tilt plots. With the blockage at the midplane, the offset viewpoint on the side where the block is present, the South side, actually cannot see the block, because it is in the shadow of the pin, so there is no reduction in the Cerenkov contributions of any segment and the value detected there is still 1.174E−7. This combined with the reduced direct viewpoint gives an adjusted tilt ratio of +0.141 for this offset, a very large apparent upwards tilt.

The two viewpoints tangential to the half channel block, the East and West views, will both have the contribution of segments 1 to 8 reduced by 50%, because they see either their left or right side of the channel blocked. These should both have the same level of detected Cerenkov of 9.82E−8, a decrease of only 16.3%. The smaller decrease is because only 1/8th of the total volume of view is blocked, because 3/4th of the visible portion of the channel is above the midplane. This decrease is larger than 12.5% because the blocked portion contains mostly middle segments, which have more gammas and electrons, resulting in greater Cerenkov contributions. Comparing the blocked value for the tangential viewpoints to the blocked direct viewpoint gives an adjusted tilt ratio

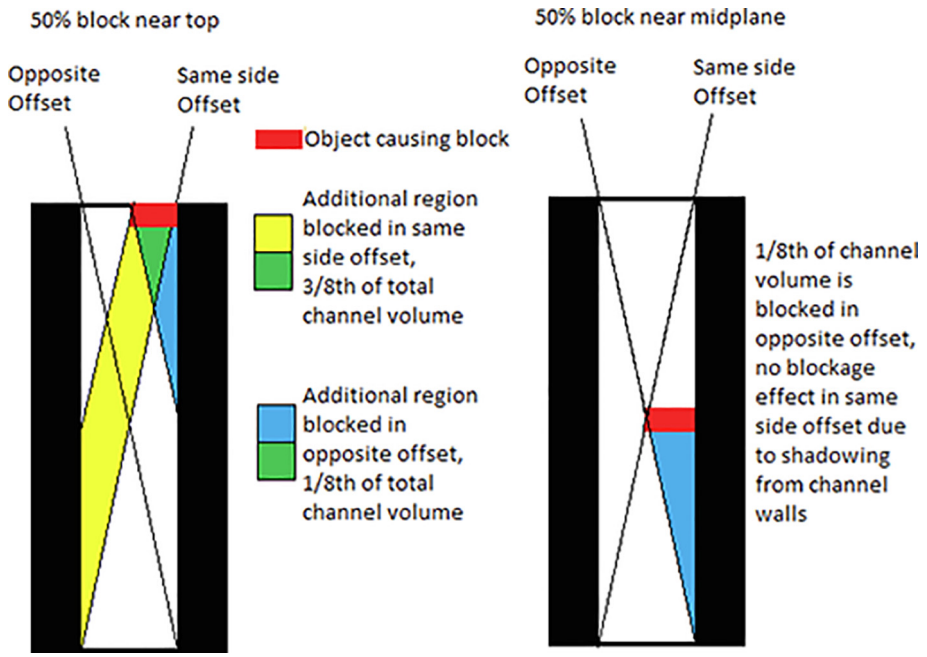

Fig. 6. Diagram demonstrating the effect that a partial block in different locations within the channel has on the offset viewpoints located on the same side and on the opposite side of the channel from the blockage.

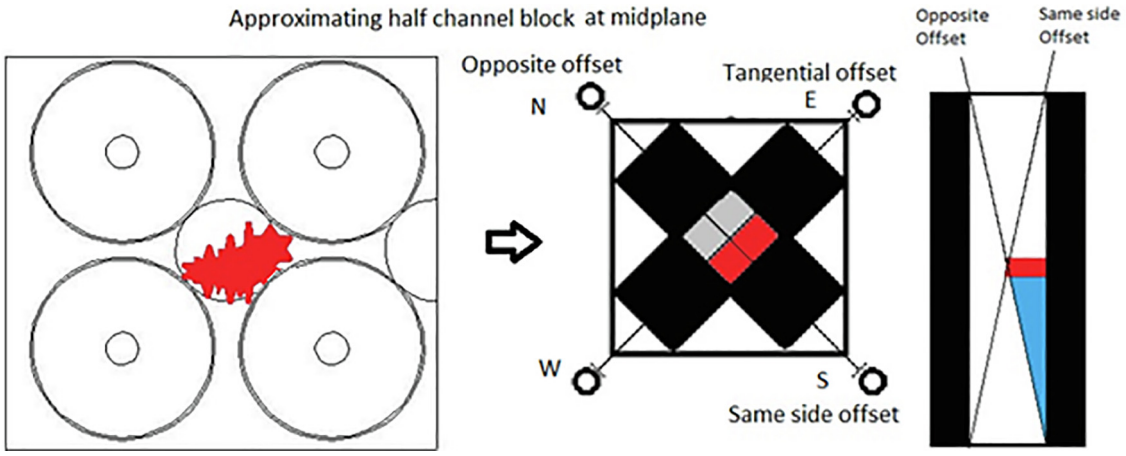

Fig. 7. Partial blockage at core midplane and its approximation for the model.

of +0.0325, a much smaller apparent upwards tilt than for the viewpoint near the midplane block.

The viewpoint opposite to the 50% midplane block, the North view, has its Cerenkov contributions from segments 1 to 8 reduced to 0, because the block covers the entire region that it can normally see below the midplane. This reduces the Cerenkov detection at this viewpoint to 7.91E−8, a decrease of 32.6%, because 1/4th of the total visible volume is blocked, and that volume is mostly comprised of segments near the middle. This makes the apparent adjusted tilt ratio −0.0762, which corresponds to a downwards tilt with a magnitude nearly 3x larger than the normal, unblocked downwards tilt for that channel. The results for each offset from the preceding section are collected and tabulated here in Table 1.

So combining the data from the direct and 4 offset detectors, the blockage causes Cerenkov detected from the direct view to be reduced by 25.4%. The offsets are reduced by 0% to the South, 16.3% to the East and West, and 32.6% to the North: this information is what is available to find out where and how large the block is. The change in 4 of the 5 viewpoints can rule out a detector malfunction, so it is assumed that all simulated measurements are accurate. It is also assumed that there is only a single blockage, because a situation with two separate blockages is far less likely and more complicated. The blockage location process could proceed as follows:

The 25.4% decrease in the direct viewpoint means that the blockage is either a 25% block near the top below segment 16, a 35% block below segment 11, a 40% block below segment 10, a 50% block at the midplane below segment 9, a 100% block somewhere within segment 6, at approximately 65% of the way down the channel, or some value in between.

The fact that there is no change in the Southern measurement means that the block must be completely within the region shadowed by the channel to the southern viewpoint, so it cannot be a block at the top, but instead must be a block smaller than or equal to the portion of the way down the channel that the block is located. So to satisfy this criteria, 25% of the way down the channel, the block must cover 25% or less of the total channel area, at the midplane it must cover 50% or less of the channel, and a full block could only occur at the bottom of the channel. Taking the possible block sizes/positions from the direct viewpoint, the information from the South rules out the possibility of a 25% block at the top, or a 100% block at ~65% of the way down the channel, but leaves the possibility of a 50% block at the midplane, located on the south side of the channel. Due to the slope of the curve for potential block sizes vs height from the direct viewpoint, the only place where it is within the region of shadow for the southern viewpoint is with a 50% block at the midplane, as anything above or below the region right around the midplane would have to be larger than the maximum size that could avoid blocking any of the southern view. Thus with only these two viewpoints, the size and location of the block in the channel can be identified.

The potential information obtainable from the other three offsets will also be mentioned here. The two tangential offsets, east and west, are both affected by the same amount, providing information that the block is symmetric with respect to the viewpoints: the line between the viewpoints is parallel to the edge of the blockage. The opposite, north, viewpoint has a larger decrease than all the others do, which shows that there is a block either on the north side near the top, or on the south side near the middle. This can provide further confirmation that it is indeed a block near the middle on the south side of the channel, because the other possibilities for creating this decrease in the north viewpoint are incompatible with the information from the other detectors.

Other sizes and positions of blocks could be determined from the Cerenkov measurements in a similar manner. A set of possible block configurations that would cause a given change in each viewpoint could be pre generated for many increments of change, and then an automated system could compare the possible configurations that would cause the response found in each viewpoint to find the blockage scenario that satisfies all of them, thus identifying the location of the block. The generation of the Cerenkov response for multiple blockage configurations using this method

Table 1
Cerenkov detection in different viewpoints with 50% block in south side of channel at core midplane.

	Direct no block	Offset no block	Direct with block	Opposite (north) offset	Same side (south) offset	Tangential (east/west) offset
Cerenkov detected	2.36E−7	1.17E−7	1.76E−7	7.91E−8	1.17E−7	9.82E−8
Adj tilt ratio	N/a	−0.0280	N/a	−0.0762	+0.1411	+0.0325
Proportional decrease in Cerenkov	N/a	N/a	0.254	0.3264	0	0.1632

is not computationally expensive to generate because the long MCNP simulation only needs to be performed once.

5. Conclusions

The detection of coolant channel blockages using a Cerenkov light measurement based power profiling system has been demonstrated. A method for determining where within a channel a blockage is located has been presented. An example blockage scenario is analyzed, and its location determined from the information obtainable from Cerenkov light detection viewpoints above the core.

CRediT authorship contribution statement

Jason A. Hearne: Conceptualization, Methodology, Software, Formal analysis, Investigation, Writing - original draft, Visualization. **Pavel V. Tsvetkov:** Supervision, Project administration, Funding acquisition, Writing - review & editing.

Declaration of Competing Interest

The authors declare that they have no known competing financial interests or personal relationships that could have appeared to influence the work reported in this paper.

Acknowledgements

This research is being performed using funding received from the DOE Office of Nuclear Energy's Nuclear Energy University Program, NEUP Award Number DE-NE0008306.

Disclaimer

This paper was prepared as an account of work sponsored by an agency of the United States Government. Neither the United States Government nor any agency thereof, nor any of their employees, makes any warranty, expressed or implied, or assumes any legal liability or responsibility for the accuracy, completeness, or usefulness of any information disclosed.

Any views, opinions, findings, conclusions, or recommendations expressed in this publication are those of the authors and do not necessarily state or reflect the views of the Department of Energy Office of Nuclear Energy

Appendix A. Supplementary data

Supplementary data to this article can be found online at https://doi.org/10.1016/j.anucene.2020.107424.

References

Adorni, M. et al., 2005. Analysis of partial and total flow blockage of a single fuel assembly of an MTR research reactor core. Ann. Nucl. Energy 32 (15), 1679–1692.

Chance, C., 2014. Partial Core Blockage Simulation Using COBRA-TF. Texas A&M University. s.l..

de Vires, J.W., van Dam, H., Gysler, G., 1990. Protection system for minimizing the consequences of a flow blockage incident at a pool-type research reactor (AECL–9926(v2)). INIS. Canada: s.n.

De Volpi, A., Fink, C.L., Stewart, R.R., 1975. Monitoring clad blockages, United States: s.n.

Greef, C.P., 1979. Temperature fluctuations: An assessment of their use in the detection of fast reactor coolant blockages. Nucl. Eng. Des. 52 (1), 35–55.

Hearne, J.A., Tsvetkov, P.V., 2020a. Three dimensional reactor power profile reconstruction using Cerenkov radiation. Ann. Nuclear Energy ANUCENE-D-19-01134. Currently under review.

Hearne, J.A., Tsvetkov, P.V., 2020b. Response function generation for Cerenkov radiation production and transport in a TRIGA coolant channel. Ann. Nucl. Energy 138 (April) 107200. https://doi.org/10.1016/j.anucene.2019.107200.

Hearne, J.A., Tsvetkov, P.V., 2020c. Spatial power profiling method using visual information in reactors with optically transparent coolants. Ann. Nucl. Energy 138 (March) 107071. https://doi.org/10.1016/j.anucene.2019.107071.

Holschuh, T., Marcum, W., 2019. The CRANK system—A simple, robust apparatus for measurement of Cherenkov light at open-pool reactor. Nucl. Technol. 8, 1–7.

Keller, F.R., 1962. Fuel element flow blockage in the engineering test reactor, United States: s.n.

Ma, Z. et al., 2018. Analysis of flow blockage accidents in rectangular fuel assembly based on CFD methodology. Ann. Nucl. Energy 112, 71–83.

Salama, A., 2012. CFD analysis of fast loss of flow accident in typical MTR reactor undergoing partial and full blockage: The average channel scenario. Prog. Nucl. Energy 60, 1–13.

Salama, A., El-Morshedy, S.E.-D., 2012. CFD simulation of flow blockage through a coolant channel of a typical material testing reactor core. Ann. Nucl. Energy 41, 26–39.

Schultheiss, G.F., 1987. On local blockage formation in sodium cooled reactors. Nucl. Eng. Des. 100 (3), 427–433.

Son, H.M., Yang, S.H., Park, C., Lee, B.C., 2015. Transient thermal–hydraulic analysis of complete single channel blockage accident of generic 10 MW research reactor. Ann. Nucl. Energy 75, 44–53.

Turkcan, E., Kozma, R., Nabeshima, K., Verhoef, J., 1992. On-Line System for Monitoring of Boiling in Nuclear Reactor Fuel Assemblies. Petten, The Netherlands, s.n.